Progress In Electromagnetics Research, Vol. 126, 169–183, 2012

ANALYSIS OF MULTI-SCALE PROBLEM ABOUT ANTENNA MOUNTED ON ELECTRICALLY LARGE PLATFORM BY USING CONNECTED EPA-PO

K. Zhang, J. Ouyang*, F. Yang, J. Zhang, and Y. Li

University of Electronic Science and Technology of China, (UESTC), China

Abstract—In this paper, a hybrid method combining equivalence principle algorithm with physical optics is proposed to solve the radiation problem of antenna mounted on electrically large platform. It is based on domain decomposition method which is a scheme for multi-scale problems. Equivalence principle algorithm can simulate antenna accurately, and physical optics is an asymptotical method to obtain current distribution on the electrically large platform. Continuity of currents is considered when the conductor on the platform is decomposed into two parts by the equivalence surface. In addition, a preconditioning for the hybridization of equivalence principle algorithm and physical optics is discussed. Numerical results demonstrate the feasibility of the hybrid method.

1. INTRODUCTION

As the antenna applications are developed rapidly, the research of antenna on electrically large platform, such as antenna on car [1, 2], on aircraft [3], and conformal antennas [4], has obtained much attention in recent years. Antenna establishes close relationships with platform. The interactions of antenna and platform cannot be ignored. Method of moments (MOM) [5–7] based on the integral equations and differential-equation-solvers, such as finite element method (FEM) [8] and finite difference in time domain (FDTD) [9], are often employed to investigate the radiation pattern of antenna on platform. However, it is time consuming and needs huge memory due to the large number of unknowns brought in the methods for the discretization of the physical

Received 13 January 2012, Accepted 7 March 2012, Scheduled 14 March 2012

* Corresponding author: Jun OuYang (antenna_ou@163.com).

geometry into cells with scales smaller than the tenth of wavelength. Furthermore, when the antenna consisting of dielectrics with high permittivity and fine structures is mounted on a large platform, some parts of the mesh are denser than the other parts. In this case, the iterative solver will converge slowly for the multi-scale feature.

Domain decomposition method (DDM), including integral equation applied in DDM (IE-DDM) [10, 11] and finite element method (FEM) applied in DDM (FEM-DDM) [12, 13], is a scheme for solving multi-scale problems. The idea of DDM is to split the whole region into several sub-regions, solve each sub-region by the most suitable method, and stitch them together. The method is flexible and requires lower computational cost.

Equivalence principle algorithm (EPA) [14–19], based on the equivalence theorem, is one kind of DDM. In this algorithm, the number of unknowns is reduced by using virtual surfaces to enclose the sub-regions. The inside unknowns are transformed to the unknowns on the equivalence surface by the equivalence theorem. The density of unknowns on the equivalence surface is smaller than that on the object with the fine structure and high permittivity. In addition, the method is good for the solution of repeated elements, such as array antennas and periodic structures, since the equivalence operator of the elements needs to be calculated and stored once. The condition number of the impedance matrix is improved by EPA. Moreover, tap-basis scheme is provided to split the conductor into two parts while keeping the continuity of currents on the surface in the case that the conductor is decomposed by the equivalence surface [20, 21].

When antenna problems with electrically large flat platform are calculated in some practical applications, the physical optics (PO) equation is competent to evaluate the currents on the platform. MOM-PO [22–24] is a typical method to solve this problem. In this method, MOM is utilized to compute the currents near the antennas and the currents on the platform are calculated by PO. Compared with MOM-PO, the hybrid method combining EPA with PO can reduce the number of unknowns since the method inherits the advantages of EPA. The rate of convergence of EPA will also be improved when PO is involved compared that in original EPA used directly. Furthermore, unlike FEM-DDM-PO [25], the proposed hybrid method avoids iterative multi-region algorithm. Therefore, the unknowns can be evaluated once.

In EPA-PO, the conductor in the outside region is isolated from the object in the inside region [26]. However, in many practical antenna applications, antennas are mounted on the platform. In Connected EPA-PO, one scheme is proposed to keep the current flowing smoothly

while cutting the conductor into two parts by the equivalence surface. The scheme refers to tap-basis scheme in EPA and MOM-PO. In addition, a preconditioning is introduced to improve the convergence of EPA-PO further. In this paper, Connected EPA-PO is utilized to solve problem about antenna mounted on large electrically large platform. The currents on antenna are modeled by EPA, while the currents on the platform are simulated by PO. Numerical results reveal the accuracy and efficiency of the proposed approach.

2. CURRENT CONTINUITY OF EPA

Based on the idea of Domain decomposition method (DDM), the whole region is divided into some sub-domains in EPA. The sub-domain which contains a large number of unknowns is enclosed by a virtual surface [14–17]. Equivalence operator (S operator) and translation operator (T operator) are involved to depict the two main procedures respectively: the scattering of objects via an equivalence surface and the interaction among the different equivalence surfaces. The equivalence operator (S) contains all information inside the surface. The detailed description of the operator can be written as in Equation (1) [14, 15]. By utilizing the S operator, unknowns on the object inside the equivalence surface can be transformed to the unknowns on the surface. The procedure can be described in Equation (2).

$$S = \begin{bmatrix} \mathbf{n}_e \times K \\ -\mathbf{n}_e \times L \end{bmatrix} [\eta L_{ss}]^{-1} [-\eta L \quad \eta K] \tag{1}$$

$$\begin{bmatrix} \mathbf{J}^{sca} \\ \frac{1}{\eta}\mathbf{M}^{sca} \end{bmatrix} = S \begin{bmatrix} \mathbf{J}^{inc} \\ \frac{1}{\eta}\mathbf{M}^{inc} \end{bmatrix} \tag{2}$$

$$\begin{aligned} K &= \frac{1}{4\pi} \int \nabla G \times \mathbf{X} d\tau \\ L &= \frac{ik}{4\pi} \int \left[\overline{\overline{I}} + \frac{1}{k^2} \nabla (\nabla \cdot \mathbf{X}) \right] G d\tau \end{aligned} \tag{3}$$

where $\mathbf{J}^{inc}$ and $\mathbf{M}^{inc}$ are the incident equivalence currents generated by the source outside the equivalence surface. $\mathbf{J}^{sca}$ and $\mathbf{M}^{sca}$ are the scattering equivalence currents replacing the electrical currents on the object to radiate electromagnetic wave. $\mathbf{n}_e$ is the outer normal vector of the surface. K and L are the integral operators shown in (3). G and η are the Green function and the wave impedance in free space. Moreover, when the elements in an antenna array are identical, the S operator needs to be calculated and stored once. The

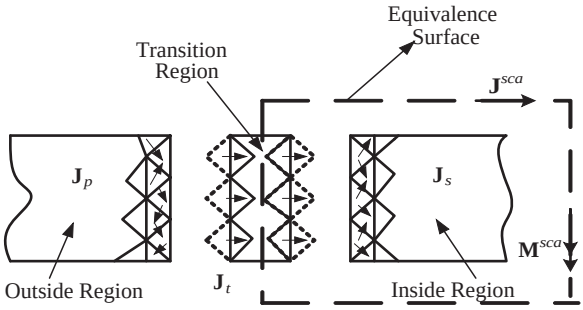

Figure 1. The strip partly enclosed by an equivalence surface is divided into three regions.

translation operator (T) describes the procedure of the interactions among different sub-regions [16, 17].

$$\begin{bmatrix} \mathbf{J}_1 \\ \frac{1}{\eta}\mathbf{M}_1 \end{bmatrix} = \begin{bmatrix} \mathbf{n}_1 \times K & \mathbf{n}_1 \times L \\ -\mathbf{n}_1 \times L & \mathbf{n}_1 \times K \end{bmatrix} \begin{bmatrix} \mathbf{J}_2 \\ \frac{1}{\eta}\mathbf{M}_2 \end{bmatrix} = T_{12} \begin{bmatrix} \mathbf{J}_2 \\ \frac{1}{\eta}\mathbf{M}_2 \end{bmatrix} \tag{4}$$

The subscripts 1 and 2 represent the equivalence surfaces 1 and 2, respectively. Like other scheme of DDM, decomposing the PEC into two parts while keeping the continuity of currents is a challenge in EPA. Currents which are continuous will be cut by the equivalence surface. The current distribution will be different from the original distribution because of the discontinuity. Hence, to eliminate the discontinuity is necessary. Tap-basis scheme [20] is utilized to tackle the problem.

In tap-basis scheme, the transition region is added. The inside region is connected by the transition region with the outside region. In Figure 1, one strip intersects with an equivalence surface. The currents are divided into three parts: $\mathbf{J}_s$ (inner currents), $\mathbf{J}_p$ (outer currents), and $\mathbf{J}_t$ (transition currents). The currents on the strip are excited by a source placed on the strip. $\mathbf{J}^{sca}$ and $\mathbf{M}^{sca}$ are the equivalence scattering currents on the surface. The basis functions at the edge of outer region and inner region belong to the transition region. The total number of basis functions is not changed hence. In EPA, the equations of this problem can be derived from electrical field equations [20] in (5).

$$\begin{cases} L_{ss}\mathbf{J}_s + L_{sp}\mathbf{J}_p + L_{st}\mathbf{J}_t = -\mathbf{E}_s^{inc} \\ L_{ps}\mathbf{J}_s + L_{pp}\mathbf{J}_p + L_{pt}\mathbf{J}_t = -\mathbf{E}_p^{inc} \\ L_{ts}\mathbf{J}_s + L_{tp}\mathbf{J}_p + L_{tt}\mathbf{J}_t = -\mathbf{E}_t^{inc} \end{cases} \tag{5}$$

The subscript s represents strip in the inside of the surface, p the strip in the outer region, and t the transition region. In antenna problems, because the excitation should be in the inner region only, $\mathbf{E}_p^{inc}$ and $\mathbf{E}_t^{inc}$

equal zero. Obviously, the contribution of far field radiation from $\mathbf{J}_s$ can be replaced by that from the scattering equivalence currents (by using S operator). Hence, the scattering equivalence currents can be written as following:

$$\begin{bmatrix} \mathbf{J}^{sca} \\ \frac{1}{\eta}\mathbf{M}^{sca} \end{bmatrix} = \begin{bmatrix} \mathbf{n}_e \times K \\ -\mathbf{n}_e \times L \end{bmatrix} \mathbf{J}_s$$
$$= \begin{bmatrix} \mathbf{n}_e \times K \\ -\mathbf{n}_e \times L \end{bmatrix} [\eta L_{ss}]^{-1} \left(-\mathbf{E}^{inc} - [\eta L \quad -\eta K]\, T_{ep}\mathbf{J}_p - L_{st}\mathbf{J}_t\right) \quad (6)$$

where

$$T_{ep} = \begin{bmatrix} -\mathbf{n}_e \times K \\ \mathbf{n}_e \times L \end{bmatrix} \quad (7)$$

$\mathbf{E}^{inc}$ is the electrical field generated by the excitation. The subscript e indicates the equivalence surface. The contribution to the currents on the equivalence surface ($\mathbf{J}^{sca}$ and $\mathbf{M}^{sca}$) consists of the contribution from the excitation, $\mathbf{J}_p$, and $\mathbf{J}_t$. The interactions between $\mathbf{J}_s$ and $\mathbf{J}_p$ can be transformed through the equivalence surface as following:

$$L_{sp}\mathbf{J}_p = [\eta L \quad -\eta K]\, T_{ep}\mathbf{J}_p \quad (8)$$

$$L_{ps}\mathbf{J}_s = T_{pe} \begin{bmatrix} \mathbf{n}_e \times K \\ -\mathbf{n}_e \times L \end{bmatrix} \mathbf{J}_s = T_{pe} \begin{bmatrix} \mathbf{J}^{sca} \\ \frac{1}{\eta}\mathbf{M}^{sca} \end{bmatrix} \quad (9)$$

where

$$T_{pe} = [\eta L \quad -\eta K] \quad (10)$$

Substituting Equations (6), (8), and (9), the Equation (5) should be written as following:

$$\begin{bmatrix} \mathbf{J}^{sca} \\ \frac{1}{\eta}\mathbf{M}^{sca} \\ \mathbf{t} \end{bmatrix} - S \begin{bmatrix} T_{ep}\mathbf{J}_p \\ \mathbf{J}_t \end{bmatrix} = \begin{bmatrix} S_{ea} \\ S_{ta} \end{bmatrix} \mathbf{J}_a \quad (11)$$

$$T_{pe} \begin{bmatrix} \mathbf{J}^{sca} \\ \frac{1}{\eta}\mathbf{M}^{sca} \end{bmatrix} + L_{pp}\mathbf{J}_p + L_{pt}\mathbf{J}_t = 0 \quad (12)$$

$$\mathbf{t} + L_{tp}\mathbf{J}_p + L_{tt}\mathbf{J}_t = 0 \quad (13)$$

where S is the equivalence operator. $\mathbf{t}$ represents the electrical field in transition region induced by $\mathbf{J}_s$ and can be defined as $\mathbf{t} = L_{ts}\mathbf{J}_s$.

Further, (11)–(13) can be written as following:

$$\begin{bmatrix} I_{ee} & 0 & -S_{ee}T_{ep} & -S_{et} \\ 0 & I_t & -S_{te}T_{ep} & -S_{tt} \\ T_{pe} & 0 & L_{pp} & L_{pt} \\ 0 & I_t & L_{tp} & L_{tt} \end{bmatrix} \begin{bmatrix} \mathbf{X}_e \\ \mathbf{t} \\ \mathbf{J}_p \\ \mathbf{J}_t \end{bmatrix} = \begin{bmatrix} S_{ea}\mathbf{J}_a \\ S_{ta}\mathbf{J}_a \\ 0 \\ 0 \end{bmatrix} \quad (14)$$

where S_{ee}, S_{et}, S_{te}, S_{tt} can be defined in (15)–(18), respectively.

$$S_{ee} = \begin{bmatrix} \mathbf{n}_e \times K \\ -\mathbf{n}_e \times L \end{bmatrix} [\eta L_{ss}]^{-1} [-\eta L \quad \eta K] \tag{15}$$

$$S_{et} = \begin{bmatrix} \mathbf{n}_e \times K \\ -\mathbf{n}_e \times L \end{bmatrix} [\eta L_{ss}]^{-1} [-\eta L_{st}] \tag{16}$$

$$S_{te} = [\eta L_{ts}] [\eta L_{ss}]^{-1} [-\eta L \quad \eta K] \tag{17}$$

$$S_{tt} = [\eta L_{ts}] [\eta L_{ss}]^{-1} [-\eta L_{st}] \tag{18}$$

$\mathbf{X}_e$ indicates the coefficient of $[\mathbf{J}^{sca}\ 1/\eta\mathbf{M}^{sca}]$, and I_{ee} and I_t represent the identity operators. By iterative solver, GMRES for instance, the coefficient of currents in the matrix Equation (14) can be calculated. Then the far field can be computed by $\mathbf{J}^{sca}$, $\mathbf{M}^{sca}$, $\mathbf{J}_t$ and $\mathbf{J}_p$. $S_{ea}\mathbf{J}_a$ and $S_{ta}\mathbf{J}_a$ are the equivalence currents induced by the electrical currents $\mathbf{J}_a$ which are generated by the excitation directly and they can be written as following:

$$S_{ea}\mathbf{J}_a = \begin{bmatrix} \mathbf{n}_e \times K \\ -\mathbf{n}_e \times L \end{bmatrix} [\eta L_{ss}]^{-1} \left[-\mathbf{E}^{inc}\right] \tag{19}$$

$$S_{ta}\mathbf{J}_a = [\eta L_{ts}] [\eta L_{ss}]^{-1} \left[-\mathbf{E}^{inc}\right] \tag{20}$$

Each equation of (11)–(13) contains the contributions of all sub-regions. Therefore, the interactions among the sub-domains are considered.

3. CONNECTED EPA-PO

In EPA, electrical field integral equation (EFIE) is used to evaluate the currents on the conductor outside the equivalence surface [14, 20]. However, when the conductor is electrically large, PEC platform for instance, the number of unknowns is considerable. In this case, EFIE will reduce the computational efficiency for two reasons: first, integral of each element requires a lot of time; second, the convergence rate of matrix is slow by using iterative solver.

In some engineering applications of antenna, sacrificing accuracy to improve efficiency is feasible. EPA-PO is a technique of taking into account both precise calculation near the antenna and efficient evaluation of electrically large objects. In EPA-PO, the inside region is called EPA region and the outside region is called PO region. The EFIE in EPA is replaced by PO Equation (21) in this region. EPA-PO can improve the condition number of the impedance matrix. The magnetic field radiated from the scattering currents on the equivalence surface can be considered as the incident magnetic field of PO region.

However, when antenna is mounted on the platform, the original EPA-PO is not competent because PO region and EPA region are isolated and the connection of the two regions is not considered. If the two regions are connected together directly, relatively large errors will be involved. Therefore, unconnected EPA-PO cannot be used directly to keep the flow of current continuous when original currents are cut by the equivalence surface.

Tap-basis scheme is introduced in connected EPA-PO. EPA region is connected by the transition region with PO region. The reason why the transition region should be added can be explained as following: first, the distance between the equivalence surface and the object in the surface is required [17]. Second, if the outside region connects with the inside region directly, the outside region will extend to the inside of the surface. According to the equivalence principle, the original sources cannot be in the same region where the equivalence sources work. Therefore, the currents on the extended part cannot be equivalent to the currents on the equivalence surface which radiate wave in the inner region. Third, PO region should be far enough away from the excitation of antenna. Otherwise, large errors will be brought.

Based on tap-basis scheme mention in section two, the Equation (12) should be rewritten as Equation (22).

$$\mathbf{J}^{PO} = 2\mathbf{n} \times \mathbf{H}^{inc} \tag{21}$$

$$-T_{pe}^{PO} \begin{bmatrix} \mathbf{J}^{sca} \\ \frac{1}{\eta}\mathbf{M}^{sca} \end{bmatrix} + \mathbf{J}_p^{PO} - T_{pt}^{PO}\mathbf{J}_t = 0 \tag{22}$$

where,

$$T_{pe}^{PO} = [2\mathbf{n}_p \times K \quad \mathbf{2n}_p \times L] \tag{23}$$

$$T_{pt}^{PO} = [2\mathbf{n}_p \times K] \tag{24}$$

$\mathbf{n}_p$ indicates the normal vector of the conductor in PO region. T_{pe}^{PO}, and T_{pt}^{PO} are the translation operators translating information from EPA region and transition region to PO region respectively. Further, the matrix Equation (14) is rewritten as (25).

$$\begin{bmatrix} I_{ee} & 0 & -S_{ee}T_{ep} & S_{et} \\ 0 & I_t & -S_{te}T_{ep} & -S_{tt} \\ -T_{pe}^{PO} & 0 & I_p & -T_{pt}^{PO} \\ 0 & I_t & L_{tp} & L_{tt} \end{bmatrix} \begin{bmatrix} \mathbf{X}_e \\ \mathbf{t} \\ \mathbf{J}_p \\ \mathbf{J}_t \end{bmatrix} = \begin{bmatrix} S_{ea}\mathbf{J}_a \\ S_{ta}\mathbf{J}_a \\ 0 \\ 0 \end{bmatrix} \tag{25}$$

In addition, it is known that the accuracy of PO will be low if the normal vector of the surface changes dramatically. In this case, the PO region should be divided into several smooth regions. The multiple reflections among the regions cannot be neglected. The translation

operator describing the mutual coupling of the regions can be defined as following:

$$T_{p^i p^j}^{PO} = [2\mathbf{n}_{p^i} \times K] \tag{26}$$

The subscript p^j and p^j represent board i and board j, and $\mathbf{n}_{pi}$ is the unit outer normal vector of board i.

4. PRECONDITIONING FOR EPA-PO

When tap-basis is involved in EPA-PO, the convergence rate becomes slow. A preconditioning is discussed to improve the condition number of the matrix in Connected EPA-PO.

The partitioned matrix L_{tt} in Equation (25) is a full rank matrix. The target of the preconditioning is using I_t to substitute L_{tt}.

$$\begin{aligned}[L_{tt}]\,\mathbf{J}_t &= [I_t]\cdot[I_t]^{-1}\cdot[L_{tt}]\,\mathbf{J}_t = [\langle \mathbf{f}_m, \mathbf{f}_n\rangle]\cdot[\langle \mathbf{f}_m, \mathbf{f}_n\rangle]^{-1}\cdot[L_{tt}]\,\mathbf{J}_t \\ &= [I_t]\cdot\left[[L_{tt}]^{-1}\cdot[I_t]\right]^{-1}\mathbf{J}_t = [I_t]\cdot\mathbf{m}\end{aligned} \tag{27}$$

Therefore,

$$\mathbf{J}_t = [L_{tt}]^{-1}\cdot[I_t]\cdot\mathbf{m} \tag{28}$$

$\mathbf{J}_t$ represents the current vector in the transition region, and $\mathbf{f}_m$ and $\mathbf{f}_n$ denote the basis functions in the transition region. $\mathbf{m}$ indicates the electrical field vector. I_t represents the identity operator. The computing time of $[L_{tt}]^{-1}$ is short for the little number of basis functions in transition region. The Equation (25) can be rewritten as following:

$$\begin{aligned}&\begin{bmatrix} I_{ee} & 0 & -S_{ee}T_{ep} & -S_{et} \\ 0 & I_t & -S_{te}T_{ep} & -S_{tt} \\ -T_{pe}^{PO} & 0 & I_p & -T_{pt}^{PO} \\ 0 & I_t & L_{tp} & L_{tt} \end{bmatrix}\cdot\begin{bmatrix} E & 0 & 0 & 0 \\ 0 & E & 0 & 0 \\ 0 & 0 & E & 0 \\ 0 & 0 & 0 & [L_{tt}]^{-1}[I_t] \end{bmatrix}\cdot\begin{bmatrix}\mathbf{X}_e \\ \mathbf{t} \\ \mathbf{J}_p \\ \mathbf{m}\end{bmatrix} \\ &= \begin{bmatrix} I_{ee} & 0 & -S_{ee}T_{ep} & -S_{et}[L_{tt}]^{-1}[I_t] \\ 0 & I_t & -S_{te}T_{ep} & -S_{tt}[L_{tt}]^{-1}[I_t] \\ -T_{pe}^{PO} & 0 & I_p & -T_{pt}^{PO}[L_{tt}]^{-1}[I_t] \\ 0 & I_t & L_{tp} & I_t \end{bmatrix}\cdot\begin{bmatrix}\mathbf{X}_e \\ \mathbf{t} \\ \mathbf{J}_p \\ \mathbf{m}\end{bmatrix} = \begin{bmatrix} S_{ea}\mathbf{J}_a \\ S_{ta}\mathbf{J}_a \\ 0 \\ 0 \end{bmatrix}\end{aligned} \tag{29}$$

E represents the unit matrix. When calculating far field, $\mathbf{J}_t$ can be computed from (28) after $\mathbf{m}$ is obtained.

5. NUMERICAL RESULTS

In this section, three examples are used to demonstrate the accuracy and efficiency of EPA-PO. The solutions are calculated by GMRES.

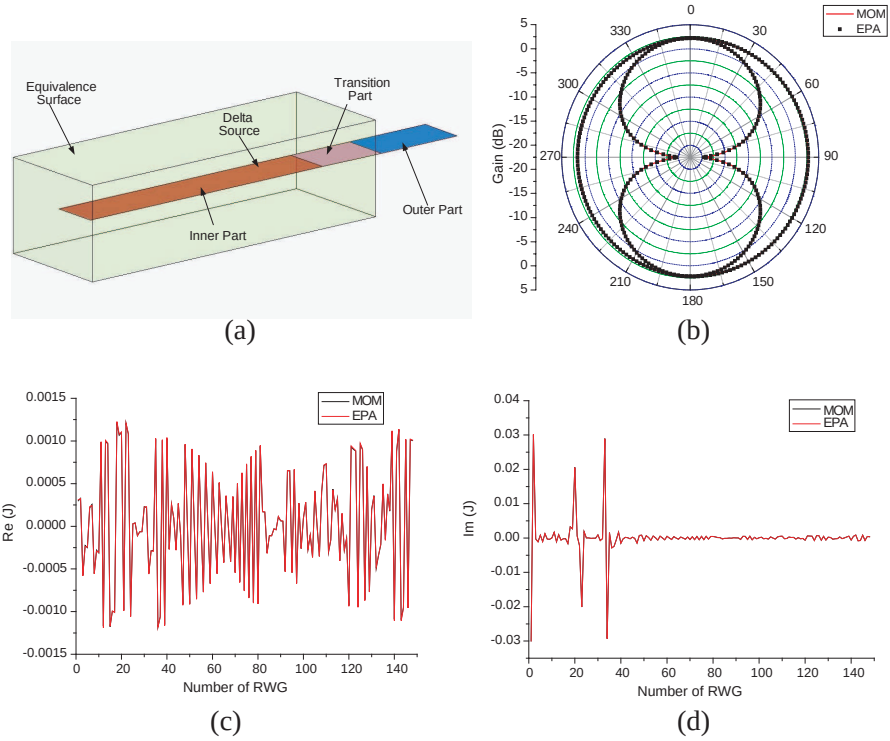

Figure 2. (a) Equivalence surface encloses one part of the dipole. (b) Radiation patter calculated by MOM and EPA. (c) Real part of current coefficients. (d) Imaginary part of current coefficients.

5.1. Test of Equivalence Principle Algorithm on Connected Region

Figure 2(a) shows one example to demonstrate the correctness of EPA on connected region. One part of the dipole is enclosed by an equivalence surface. The length of the dipole is $\lambda_0/2$. λ_0 is the wavelength in free space. The whole antenna is divided into three parts. The transition part connects the inside part and outside part. The size of the surface is $0.39\lambda_0 \times 0.13\lambda_0 \times 0.10\lambda_0$. The size of the each part is $0.32\lambda_0$ for inner part, $0.08\lambda_0$ for transition part and $0.10\lambda_0$ for outer part respectively. Delta gap excitation at 4 GHz is added at the center of the dipole. The antenna and the surface are modeled by RWG basis functions. The radiation pattern and the current value of EPA are compared with method of moments (MOM). The results shown in Figures 2(b), (c) and (d) prove that the tap basis scheme keeps the accuracy of EPA on connected region.

5.2. Patch Antenna Mounted on Electrically Large Plane

The radiation of one patch antenna placed on a ground plane with the scale of $6\lambda_0 \times 6\lambda_0$ is investigated. The antenna works at 4 GHz. The entire region consists of antenna region, transition region and platform region shown in Figure 3(a). One virtual surface encloses the antenna region. The size of surface is about $0.88\lambda_0 \times 0.88\lambda_0 \times 0.23\lambda_0$. The relative dielectric permittivity ε_r is 2.2. The thickness of the substrate is about $0.027\lambda_0$. The sizes of the patch and the substrate are $0.31\lambda_0 \times 0.31\lambda_0$ and $0.43\lambda_0 \times 0.43\lambda_0$ respectively. The mesh on antenna is dense in order to ensure the accuracy. By considering that change of currents in platform region is not as dramatic as that in antenna region, the size of mesh in platform region could be relatively large. Therefore the contrast ratio of mesh is about 4 in the whole problem. The iterative solver works in low efficiency. The width of

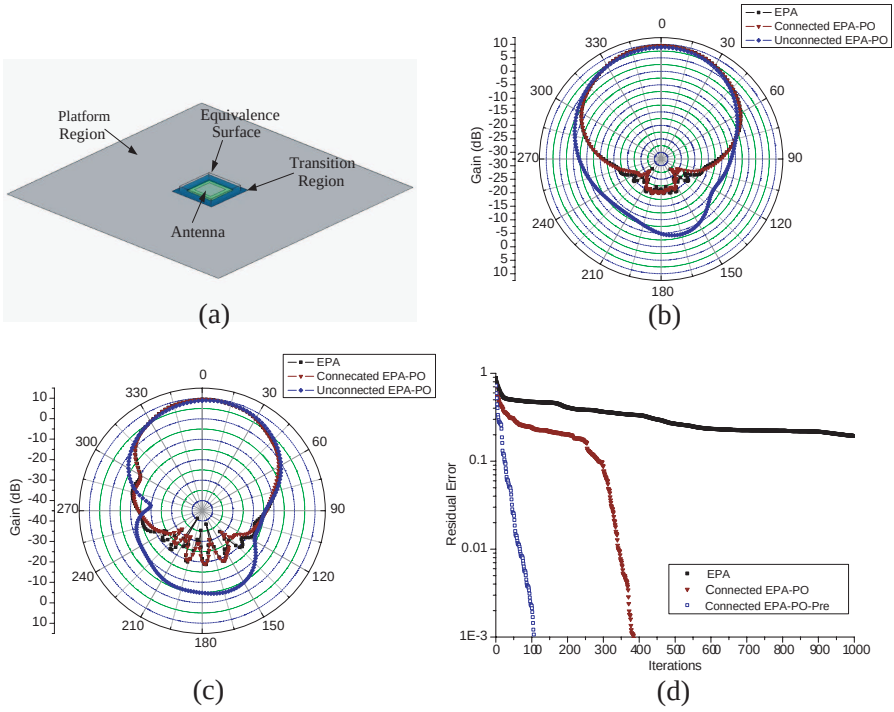

Figure 3. (a) One patch antenna mounted on an electrically large platform. (b) E-plane radiation pattern. (c) H-plane radiation pattern. (d) Comparison of convergence between EPA, EPA-PO and EPA-PO-Pre.

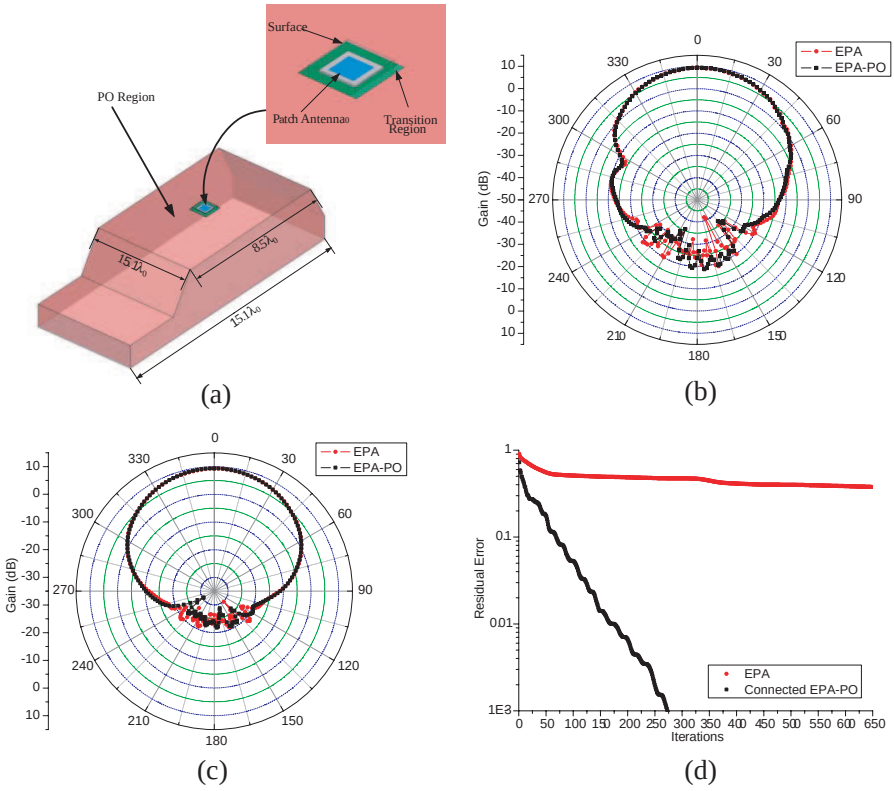

Figure 4. (a) Model of one patch antenna on the roof of a car. (b) E-plane radiation pattern. (c) H-plane radiation pattern. (d) Comparison of iterations between EPA and EPA-PO.

transition region is about $0.2\lambda_0$. The number of unknowns in the three regions is 2865 for antenna region, 304 for transition region, and 2458 for platform region respectively. After EPA is involved, the number of unknowns in antenna region reduces to 1332. Figures 3(b) and (c) reveal the results of radiation pattern. It is clear that the accuracy of EPA-PO on connected region is acceptable. The direct connection of EPA region and PO region brings relative large errors. Therefore adding transition region in EPA-PO is valid. RMS error of the lobe ($0^\circ \sim 120^\circ$, $240^\circ \sim 360^\circ$) in E plane and H plane are 1.01 dB and 0.71 dB respectively. Figure 3(d) shows that convergence rate of EPA is slow and connected EPA-PO method is much faster. In addition, the preconditioning scheme mentioned before improves the convergence of EPA-PO further.

5.3. Radiation of Patch Antenna Placed on the Complicated Electrically Large Platform

In this example, EPA-PO is utilized to solve the problem in practical application. One patch antenna is mounted on the roof of a car which can be considered as a complicated electrically large platform. The details of the car are ignored in this model. The size of the car is shown in Figure 4(a). The patch is working at 1.5 GHz. The relative dielectric permittivity ε_r is also 2.2. The thickness of the substrate is about $0.01\lambda_0$. The sizes of the patch and the substrate are $0.32\lambda_0 \times 0.32\lambda_0$ and $0.50\lambda_0 \times 0.50\lambda_0$ respectively. EPA can reduce the number of unknowns of the antenna by using one virtual surface to enclose the patch. The dimension of EPA matrix equation is about 41% of the MOM one in the antenna region. In addition, the accuracy of PO will be kept in the problems with smooth surface. However, in this example, the normal vector of the surface changes dramatically at some places. Therefore, as discussed before, the PO region should be divided into several parts and the interactions among different parts should be considered. The radiation pattern and iterations of EPA and EPA-PO are compared in Figure 4(b), Figure 4(c) and Figure 4(d) respectively. It is obviously that the results of EPA-PO are in acceptable agreement with those calculated by EPA. Moreover, EPA-PO with the preconditioning only needs less than 300 iterations to converge to the relative residual error of 0.001.

6. CONCLUSION

In this paper, connected EPA-PO is proposed to solve the radiation problem of antenna on electrically large platform. Both precise calculation near the antenna and efficient evaluation of electrically large objects are taken into account in this method. The number of unknowns in antenna region is reduced due to the characteristics of EPA, and the convergence is improved when PO is involved. The scheme of keeping the flow of currents continuous in EPA-PO is discussed. Moreover, a preconditioning is used to improve the convergence of EPA-PO further. The numerical results demonstrate the feasibility of the hybrid method in application.

ACKNOWLEDGMENT

This work was supported by the postdoctoral Science Foundation of China (Nos. 20090461325, 201003690), GADF (No. 9140A01020109DZ0202), the National Natural Science Foundation of China (Nos. 61001029,10876007),

the Fundamental Research Funds for the Central Universities (No. 103.1.2 E022050205).

REFERENCES

1. Wu, P., J. Pei, and G. Liang, "A novel super thin planar car antenna," *IEEE International Conference on Microwave and Millimeter Wave Technology*, 377–379, 2010.
2. Hsu, H.-T., F.-Y. Kuo, and H.-T. Chou, "Convergence study of current sampling profiles for antenna design in the presence of electrically large and complex platforms using fit-UTD hybridization approach," *Progress In Electromagnetics Research*, Vol. 99, 195–209, 2009.
3. Byun, G., C. Seo, B. J. Jang, and H. Choo, "Design of aircraft on-glass antennas using a coupled feed structure," *IEEE Trans. Antenn. Propag.*, No. 99, Jan. 2012.
4. Wang, X., M. Zhang, and S.-J. Wang, "Practicability analysis and application of PBG structure on cylindrical conformal microstrip antenna and array," *Progress In Electromagnetics Research*, Vol. 115, 495–507, 2011.
5. Zhao, X. W., X. J. Dang, Y. Zhang, and C. H. Liang, "The multilevel fast multipole algorithm for EMC analysis of multiple antennas on electrically large platforms," *Progress In Electromagnetics Research*, Vol. 69, 161–176, 2007.
6. Xia, L., C.-F. Wang, L.-W. Li, P.-S. Kooi, and M.-S. Leong, "Resonant behaviours of microstrip antenna in multilayered media: An efficient full-wave analysis," *Progress In Electromagnetics Research*, Vol. 31, 55–67, 2011.
7. Lim, C.-P., "Method of moments analysis of electrically large thin square and rectangular loop antennas: Near-and-far-zone field," *Progress in Electromagnetics Research*, Vol. 34, 117–141, 2001.
8. Trujillo-Romero, C. J., L. Leija, and A. Vera, "FEM modeling for performance evaluation of an electromagnetic oncology deep hyperthermia applicator when using monopole inverted T, and plate antennas," *Progress In Electromagnetics Research*, Vol. 120, 99–125, 2011.
9. Lei, J.-Z., C.-H. Liang, W. Ding, and Y. Zhang, "EMC analysis of antennas mounted on electrically large platforms with parallel FDTD method," *Progress In Electromagnetics Research*, Vol. 84, 205–220, 2008.
10. Peng, Z., X.-C. Wang, and J.-F. Lee, "Integral equation based domain decomposition method for solving electromagnetic wave

scattering from non-penetrable objects," *IEEE Trans. Antenn. Propag.*, Vol. 59, No. 9, Sep. 2011.

11. Peng, Z., X.-C. Wang, F.-R. Lei, J.-F. Lee, "Integral equation based domain decomposition method for electromagnetic wave scattering problems," *IEEE EMTS/URSI*, 624–627, Aug. 2010.
12. Lu, Z.-Q., X. An, and W. Hong, "Substructure DDM with vector FEM for 3-D electromagnetic scattering problems," *Microwave Conference Proceedings*, Vol. 3, 3, 2005.
13. Liu, P. and Y.-Q. Jin, "The finite-element method with domain decomposition for electromagnetic bistatic scattering from the comprehensive model of a ship on and a target above a large-scale rough sea surface," *IEEE Trans. Geoscience and Remote Sensing*, Vol. 42, No. 5, May 2004.
14. Li, M.-K. and W. C. Chew, "Wave-field interaction with complex structures using equivalence principle algorithm," *IEEE Trans. Antenn. Propag.*, Vol. 55, No. 1, 130–138, Jan. 2007.
15. Sun, L.-E., M.-K. Li, and W. C. Chew, " Applying the low frequency technique to the equivalence principle algorithm," *Antenna and Propagation Society International Symposium*, 1–4, 2009.
16. Li, M.-K. and W. C. Chew, "A domain decomposition scheme based on equivalence theorem," *Micro. Opt. Tech. Lett.*, Vol. 48, No. 9, 1853–1857, Sep. 2006.
17. Shao, H., J. Hu, Z. Nie, G. Han, and S. He, "Hybrid tangential equivalence principle algorithm with MLFMA for analysis of array structures," *Progress In Electromagnetics Research*, Vol. 113, 127–141, 2011
18. Yla-Oijala, P. and M. Taskinen, "Solving electromagnetic scattering by large and complex structures with surface equivalence principle algorithm," *Waves in Random and Complex Media*, Vol. 19, No. 1, Feb. 2009.
19. Yla-Oijala, P. and M. Taskinen, "Solving electromagnetic scattering by multiple targets with surface equivalence principle algorithm," *3rd European Conference on Antenna and Propagation*, 88–92, Mar. 2009.
20. Li, M.-K. and W. C. Chew, "Multiscale simulation of complex structures using equivalence principle algorithm with high-order field point sampling scheme," *IEEE Trans. Antenn. Propag.*, Vol. 56, No. 8, 2389–2397, Aug. 2008.
21. Li, M.-K. and W. C. Chew, "Using tap basis to implement the equivalence principle algorithm for domain decomposition in

integral equations," *Micro. Opt. Tech. Lett.*, Vol.48, No. 11, 2218–2222, Nov. 2006

22. Zong, X. Z., Z. P. Nie, S. Yan, and S. Q. He, "Application of the PE-basis function in hybrid MOM-PO methods," *IEEE Antenna and Propagation Society International Symposium*, 1–4, 2008.
23. Zhao, X.-W., Y. Zhang, and H.-W. Zhang, "Parallel MOM-PO method with out-of-core technique for analysis of complex arrays on electrically large platforms," *Progress In Electromagnetics Research*, Vol. 108, 1–21, 2010.
24. Hu, B., X. Xu, M. He, and Y. Zheng, "More accurate hybrid PO-MOM analysis for an electrically large antenna-radome structure," *Process In Electromagnetics Research*, Vol. 92, 255–265, 2009.
25. Jin, Z., K. Zhao, P. H. Pathak, J. Zou, and J.-F. Lee, "A hybrid FEM-DDM-PO method for electrically large objects," *IEEE Antenna and Propagation Society International Symposium*, 5909–5912, Dec. 2007.
26. Zhang, K. Z., J. Zhang, J. Ouyang, and F. Yang, "A novel hybrid method with equivalence principle algorithm and physical optics for antenna problem on electrically large platform," *IEEE AP-S/URSI*, 2530–2532, 2011.